

Influence of Ply Stacking Sequences on the Impact Response of Carbon Fibre Reinforced Polymer Composite Laminates

Kristian Gjerrestad Andersen
*School of Engineering and Computer
Science*
University of Hertfordshire
Hatfield, UK
kristiangander@gmail.com

Gbanaibolou Jombo
*School of Engineering and Computer
Science*
University of Hertfordshire
Hatfield, UK
g.jombo@herts.ac.uk

Sikiru Oluwarotimi Ismail
*School of Engineering and Computer
Science*
University of Hertfordshire
Hatfield, UK
s.ismail3@herts.ac.uk

Segun Adeyemi
University of Hertfordshire
Hatfield, UK
s.s.adeyemi@herts.ac.uk

Rajini Nagarajan
*Department of Mechanical Engineering
Kalasalingam Academy of Research
and Education*
Tamil Nadu, India
rajiniklu@gmail.com

Sufyan Akram
*School of Engineering and Computer
Science*
University of Hertfordshire
Hatfield, UK
s.akram3@herts.ac.uk

Abstract— In recent years, there has been a growing demand for high strength-to-weight ratio and lightweight structures in several applications, such as wind energy, automotive, aerospace, telecommunication and construction industries. Carbon fibre reinforced polymeric (CFRP) composite is one of the promising materials with aforementioned inherent properties and applications. These properties vary with different techniques of their manufacturing, such as stacking sequence. Hence, it is germane and important to conduct an extensive study to investigate the effect of stacking sequences on the properties of CFRP composites. Consequently, this paper experimentally investigated the influence of different ply stacking sequences on quasi-static low-velocity impact behaviour of approximately 150 x 130 x 2 mm CFR epoxy composite laminates, manufactured by hand lay-up technique. Five different stacking sequences, denoted as samples A, B, C, E and F were tested under impact loads of 2.00, 2.25 and 2.50 kN. The results showed that the Sample A with stacking sequence of $[90/\pm 45/0]_s$ exhibited the highest impact resistance under a maximum load of 2.50 kN before it finally fractured at a maximum displacement of nearly 10.20 mm, prior to an inter-ply delamination occurrence at displacement of approximately 5.50 mm. Similarly stacked sample B recorded the lowest inter-ply delamination damage, while sample C exhibited highest delamination damage. Both samples E and F exhibited similar impact properties. Moreover, samples A, B and C absorbed impact energies of 17.50, 6.25 and 14.13 J, respectively. Conclusively, sample A with highest impact resistance and absorbed energy is hereby recommended, been a promising material for engineering application within the test conditions and parameters, especially under a low-velocity impact load.

Keywords—*stacking sequences, low-velocity impact, impact energy absorbed, inter-ply delamination, impact damage.*

I. INTRODUCTION

As composite materials, such as carbon fibre reinforced polymer (CFRP) types, are increasingly finding their applications in wind energy, aerospace, automotive, construction, telecommunication military and other structures due to their light weight and high specific strength, the need arises to optimise their lay-up to be more resilient against damage modes in operation.

To address this challenge, several studies have considered damage mode in CFRP composites, using different approaches: experimental, analytical and numerical approaches, among others. From the experimental point of view, parameters such as fibre volume fraction, fibre orientation, curing temperature and processing method have been varied to study their effects on enhancing composite mechanical properties (tensile strength, hardness, among others) and thermal properties [1–6]. On the other hand, numerical approach generally involves global lay-up stacking optimisation considering either buckling resistance to compressive load, manufacturing constraints or natural frequency consideration [7–10].

Low-velocity impact could be from flying pebbles or stones, ices/hails, birds, among other solid objects on the road sides, run ways and in the sky. CFRP composites with different ply stacking sequences (based on various fibre orientations) have different level of damage mode, when low-velocity impact. Several works have been recently reported on responses of CFRP composites to low-velocity impact energy [11–13]. However, studies on effects of stacking sequences of CFRP composites laminates on impact response are rare and scanty.

Therefore, this present paper focuses on the influence of quasi-isotropic CFRP composite ply stacking sequences on low-velocity impact response. An experimental approach is adopted, with two parameters (impact response as a function of load *versus* displacement and energy absorbed) to characterise the impact behaviour of the composite laminates. Five different composite laminate samples with varied ply stacking sequences; based on fibre orientations are studied. Importantly, this investigation has the potential of benefiting all designers, manufacturers and users of CFRP composite laminates by guiding and giving relevant information on material selection: optimal laminate with most suitable ply stacking sequence and maximum low-velocity impact resistance property in application.

II. MATERIALS AND METHOD

A. Sample Preparation

The CFRP composite laminates consist of prepregs were used in this experiment. They were made up of seven different stacking sequences, as shown in Table I. The samples were manufactured by hand lay-up technique. Prepreg stands for pre-impregnated composite fibre, where a thermoset polymer matrix material (epoxy resin) was used to bond the carbon fibres together during manufacturing. An advantage of using prepregs over conventional woven composite sheets (dry reinforcements) including prepregs already have their carbon fibres filled with resin and hardener; the resin was already combined with the carbon fibres. The prepregs were placed directly into the mould, without the need to handle wet resin in a resin infusion process. The curing of the prepreg laminates started after they have been heated, normally in an autoclave machine.

TABLE I. TEST SAMPLE CONFIGURATION

Test Sample	Material	Stacking Sequence	Dimensions (mm)	Laminate Type
A	FibreDUX 6268C-HTA 12K	$[90/\pm 45/0]_s$	150x135x2	Quasi-Isotropic
B	FibreDUX 6268C-HTA 12K	$[90/0/\pm 45]_s$	150x135x2	Quasi-Isotropic
C	FibreDUX 6268C-HTA 12K	$[90/0]_{2s}$	150x135x2	Quasi-Isotropic
E	FibreDUX 6268C-HTA 12K	$[90_3/0_3]_s$	150x135x2	Quasi-Isotropic
F	Hexcel G803 3K 5H	$[0/\pm 45/90]_s$	150x135x2	Quasi-Isotropic

The roll of prepregs was kept inside a polythene bag after being manufactured, before putting it in a freezer. Before the samples were put into layers, they were thawed for five hours in order to obtain ambient temperature. The thawing was made while the prepregs were still in the polythene bag, as condensation on the surface of the material would impact the material properties and appearance of the laminate. After thawing, the prepregs were cut and plied in their respective orientations, as indicated in TABLE I. A wooden roller was regularly used across the surface in order to evict any trapped air in the material and ensure that the desired shape was reached. The lay-up of prepregs used for the manufacturing of the CFRP composite laminates was pressurised at 90 kPa overnight [14].

Next, during vacuum bagging process, the lay-up was covered in nylon 6/6 vacuum bagging film of VAC-PAK HS6262 type. This particular film was chosen because of its high temperature and pressure resistance, which are needed during curing stage. The prepreg laminates were moulded into its form using an aluminium plate, with release films to avoid sticking on the top and bottom of the laminates, as depicted in Fig. 1. After putting on the release films, two layers of breather were placed on top in order to allow a good escape route for the air inside the vacuum bag, when the pumping commenced. The breather was typically a woven polyester/polyamide felt fabric with a relatively high curing temperature, depending on the chosen curing temperature; generally between 100-200 °C. Additionally, gases that were

produced during the curing cycle were evacuated through the breather. Then, the sealant tape was added 10 mm away from the laminate, the vacuum bag was used to cover the entire set-up and the vacuum pump was set-up. Finally, the vacuum bag with its contents were placed in the autoclave machine (Fig. 2).

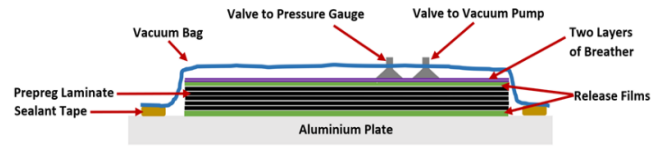


Fig. 1. The vacuum bagging of the test sample, during preparation.



Fig. 2. The autoclave machine used during sample preparation.

Inside the autoclave machine, the curing cycle shown in Fig. 3 was used. This cycle was used to ensure a satisfactory surface quality and even temperatures distribution across the laminate to give a little or negligible difference between the temperature of the components and heat source. The ambient starting temperature was 20 °C, the rate of heating was 1 °C/min. The assembly was heated up to 121 °C before being given two hours of curing time at this temperature with a pressure of 106 kPa. Thereafter, the laminate was allowed to cool until an ambient temperature was regained.

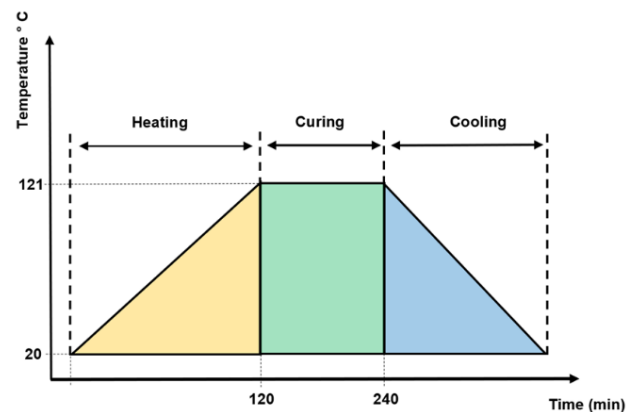


Fig. 3. The autoclave curing cycle used.

After the curing cycle was completed and the laminates regained ambient temperature, the finished CFRP laminates were removed from the bag. Then, the laminate samples were cut into the dimensions of approximately 150 x 135 mm with a waterjet cutting machine, ready for the low-velocity impact tests, as designed. The following set of samples were used: 4 x sample A, 4 x sample B, 4 x sample C, 2 x sample E and 2

x samples F. Furthermore, the samples were designated with numbers 0-3, where 0 represented non-impacted samples and other 3 samples were impacted. Analysis of average of three samples was used to report the results obtained, to ascertain consistency and repeatability and accuracy. For example, the same samples A were designated as A0, A1, A2 and A3, with an increasing impacting force serially. The samples E and F were simply named as 0 and 1, where sample 0 was non-impacted and 1 was subjected to the middle level of impact load; equivalent to the impact force on samples A2, B2 and C2.

B. Experimental Set-up

A low-velocity impact experiment was performed on a Tinius Olsen Model 25ST Universal Benchtop Tester, as shown in Fig. 4. This model has a maximum loading capacity of 25 kN. The force/displacement measurements were taken on the machine with its in-built strain gauge-based load cells, having accuracy of $\pm 0.2\%$, and an extensometer with an accuracy of $\pm 10 \mu\text{m}$. The machine produced real-time measurements which were displayed on a force-displacement graph through the Horizon, a computer-assisted data-acquisition/machine control system. After the experiment was completed, a complete dataset was retrieved from the machine and imported to an Excel format, which were further processed in programming environment, such as Python, to obtain the loading curves only.



Fig. 4. Tinius Olsen Model ST25.

The machine consists of a hemispherical indenter with diameter of 25.4 mm and four toggle clamps attached to a steel plate, as shown in Fig. 5. The steel clamp has a machined slot in the middle section to give the impacted area space to deform or fracture during the impact testing.

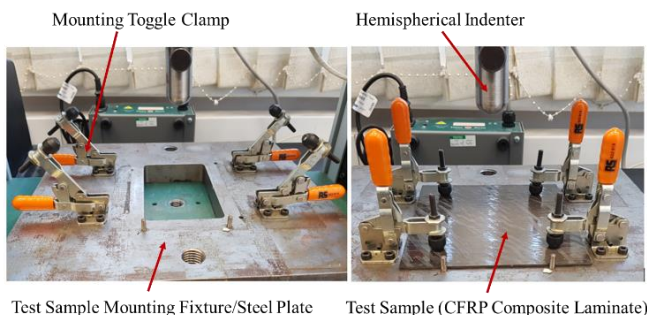


Fig. 5. Low-velocity impact test set-up.

All the tested samples were impacted with a velocity of 2 mm/s required for a low-velocity impact test [14]. The first sample A1, A2 and A3 were impacted under maximum loads of 2.00, 2.25 and 2.50 kN, respectively. The selection of the loads used was based on previous experience, preliminary tests conducted and [14]. This procedure was repeated on all sets of the test samples, except for samples E and F with 2 samples per set. Samples E0 and F0 remain non-impacted, as a reference sample. While, sample E1 and F1 were subjected to average maximum load of 2.25 kN.

III. PHYSICS OF IMPACT-INDUCED DAMAGE

In metals, low-energy impact damage is not usually considered to be a serious safety risk as the inherent ductility and force absorption capabilities of metals, such as iron, will not affect the overall structural integrity of the material [15]. However, fibre reinforced polymeric composites, such as CFRP types do not possess the same ductility in their structure and hence, they are highly brittle materials, implies that that energy is only absorbed in the elastic loading zone before damage occurs, when the elastic limit is exceeded.

According to Andrew et al. [15], there are five phases of damage in CFRP composite laminate. They occur in the following order as the impact force on the CFRP laminate sample is increased:

1. Matrix cracking and fibre matrix de-bonding.
2. Transverse bending crack as a result of high flexural stress on the opposite side of the impacted zone.
3. Inter-laminar delamination.
4. Fibre failure, caused by micro buckling under compression loading.
5. Penetration, if there is no re-bouncing of impactor.

It is evident that matrix cracking and inter-laminar delamination are the early damage signs of a low-energy impact load on a composite material. However, distinguishing the effect of either low-energy or high-energy impact loads has no set threshold limit for occurrence of the damage mechanism or phase in CFRP composite laminates. This depends on several factors, which include but are not limited to, thickness of the sample, stacking sequence of ply, fibre volume fraction, fracture toughness of resin and curing process [6,15]. Moreover, provided there are no manufacturing flaws, such as cavities or porosity in the material, or uneven distribution of the resin filler material. This could also affect the damage mechanism of the composite laminate.

IV. RESULTS AND DISCUSSION

The results obtained from the low-velocity tests are shown in Figs. 6–9, after extracted from the Horizon software as a comma separated values file and processed with Python software programme to obtain the loading curves only. The test results for all the samples that were subjected to the same maximum load were plotted together. Therefore, Fig. 6 shows the load-displacement curve for samples A1, B1 and C1, under maximum impact load of 2.00 kN.

Considering Fig. 6, there were hints of initial failures, causing a small drop in force at few certain displacements. In sample A1 failure began earliest at around displacements of 2.9, 3.9 mm and 4.2 mm. This phenomenon was caused due

to the kink-band development [15], and it could be traced to an audible “pop” sound that was heard during the impact test. Kink band caused a sudden drop in load as the surface, middle and back of the sample buckled, sheared and torn slightly under a compressive force, shear and tensile stresses, respectively.

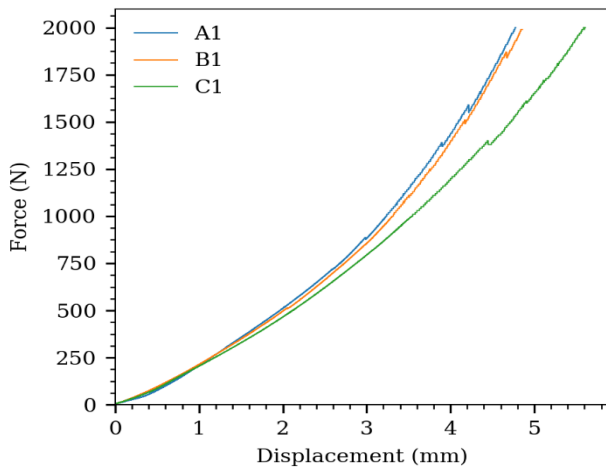


Fig. 6. Impact response of samples A1, B1 and C1 under maximum load of 2.00 kN.

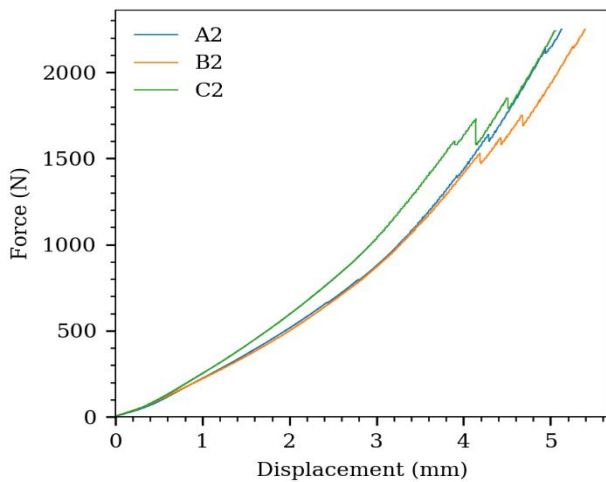


Fig. 7. Impact response of samples A2, B2 and C2 under maximum load of 2.25 kN.

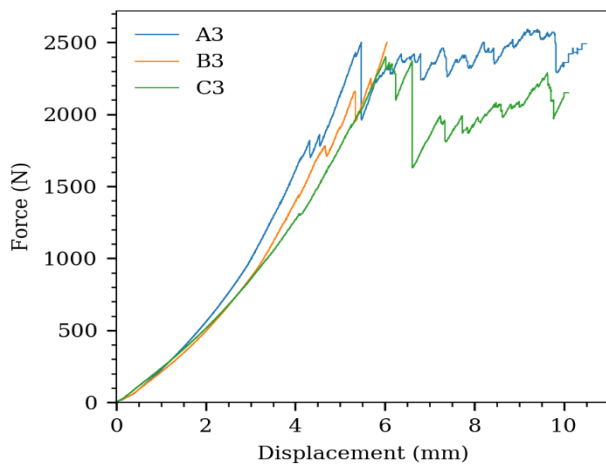


Fig. 7. Impact response of samples A3, B3 and C3 under maximum load of 2.50 kN.

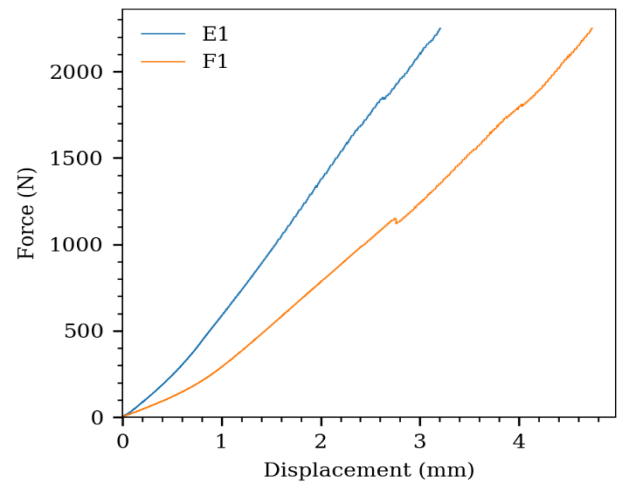


Fig. 8. Impact response of samples E1 and F1 under average maximum load of 2.25 kN.

Moreover, there was a lateral displacement of the fibres in the impacted zone, causing a barely visible impact damage (BVID). As the indenter moved into the sample, load continued to rise until the next “pop” was heard due to formation of another kink-band. This trend was similar to the other two samples B1 and C1. But, sample C1 recorded the highest elongation or displacement of nearly 5.60 mm, when compared with samples B1 and C1 of nearly 4.80 mm. It was evident that all the three samples recorded similar response to maximum impact force of 2.00 kN, but different displacements. Therefore, a higher material displacement was possible with sample A1 with stacking sequence of $[90/0]_{2s}$ than $[90/\pm 45/0]_s$ and $[90/0/\pm 45]_s$ of sample B1 and C1, respectively.

As the load was increased to 2.25 kN for samples A2, B2 and C2 (Fig. 7), there were significant similar load drops and displacement across the three samples than what was observed on 2.00 kN. These larger load drops could be potentially a sign of a more serious damage characteristics, such as initial inter-ply delamination caused by matrix cracks, being restricted and led between two layers of the laminates.

Furthermore, Fig. 8 depicts a significant material failure for the three samples A3, B3 and C3, under a maximum impact force of 2.50 kN. Evidently, Sample A3 exhibited the highest impact resistance at maximum load of 2.50 kN before it finally fractured at a maximum displacement of nearly 10.20 mm, after inter-ply delamination occurred at displacement of approximately 5.50 mm. Sample B3 recorded the lowest inter-ply delamination damage before fracture or rupture occurred at a lowest displacement of nearly 6.00 mm. The largest-scale delamination was recorded by sample C3 at displacement value of 6.50 mm (Fig. 8). Sample C3 later failed after a displacement of 10.00 mm. After this point, there was sequentially more matrix cracking, carbon fibre breakage, fibre de-bonding and eventually, a complete fracture of the integrity of the CFRP composite material. The failure mode of both samples A3 and C3 was similar, especially their delamination damage. However, sample C3 experienced nearly a full loss of material integrity under an impact load of 2.37 kN. It was evident that stacking sequence of $[90/\pm 45/0]_s$ in sample A3 exhibited a highest impact force resistance, while similar stacking sequence of $[90/0/\pm 45]_s$ in sample B3 recorded a maximum inter-ply delamination resistance property. These results could be attributed to the uneasiness of impact load and cracks to propagate within laminates of

different fibre orientations of 90, 0, +45 and -45 degrees; higher impact energy and cracks were absorbed and arrested, respectively, as similarly reported [16].

More also, sample E1 and F1 were slightly thicker than other samples, due to their stacking sequence systems. But, it was still approximately 2 mm. Both samples E1 and F1 were subjected to an average impact load of 2.25 kN. The load-displacement curve was observed (Fig. 9), which resembled the smaller kink-bands earlier observed in the samples A1, B1 and C1 under impact load of 2.00 kN. There are three factors that might have affected this phenomenon: material, thickness and ply sequence. The material for sample F1 was of a different type (Hexcel G803 3K 5H), compared with samples A, B, C and E which were all made up of FibreDUX 6268C-HTA 12K material (Table I). However, sample E of the same material with samples A, B and C. Therefore, it is more likely that the difference in the results obtained from samples E and F could be traced to their slightly thicker dimension, when compared with other samples A2, B2 and C2 under same average load of 2.25 kN.

In addition, to obtain approximated values of the energy absorbed by the impacted similar samples A, B and C under maximum impact loads of 2.00, 2.25 and 2.50 kN, the trapezoidal rule was applied to the datasets. The trapezoidal rule approximated the area below the load-displacement curve, by calculating and summarising the area of $n-1$ trapezoids below the curve in a dataset containing n data points. The rule can be defined using (1).

$$E = \frac{1}{F} \int_b^a f(x) dx \approx \sum_{n=1}^N \frac{(f(x_{n-1}) + f(x_n))}{2} * \Delta x_n \quad (1)$$

where E is the energy absorbed, F is the load, a and b are the lower and upper limits of integration, respectively, $f(x)$ is the position of the y -axis (load) with regards to the x -axis (displacement), n represents each data point in the dataset obtained from each impacted sample.

Therefore, Fig. 9 shows the variation of the impact energy absorbed by the various test samples in response to the low-velocity impact input.

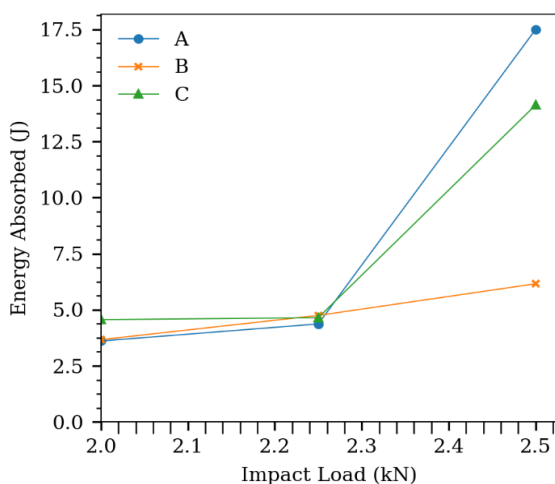


Fig. 9. Variation of impact energy absorbed by the CFRP composite test samples A, B and C under maximum impact loads of 2.00, 2.25 and 2.50 kN.

From the results obtained on impact energy absorbed, samples A and B absorbed nearly same impact energy of

approximately 3.75 J, while sample C recorded approximately 4.40 J under same impact load of 2.00 kN. The absorbed energy of samples A and B increased to nearly 4.40 J, as that of sample C remained unchanged under an increased average maximum impact load of 2.25 kN. However, the three samples absorbed more energy under a maximum impact load of 2.50 kN. Sample A, B and C absorbed impact energies of 17.50, 6.25 and 14.13 J, respectively. The highest value of energy absorbed by sample A was connected with its stacking sequence and directly linked to the failure of structural integrity in the sample. Importantly, sample B was only sample that did not show signs of material failure in form of delamination and fibre breakage. This has been earlier explain, using Fig. 8. Therefore, it can further observed and confirmed through its relatively lowest energy absorption, when compared with samples A and C.

V. CONCLUSIONS

The effects of various ply stacking sequences on the quasi-static low-velocity impact response of CFRP composite laminates have been studied. Based on the experimental results obtained within the test parameters and conditions used, the following concluding remarks are subsequently stated.

- It was evident that stacking sequence of $[90/\pm 45/0]_s$ in sample A exhibited a highest impact force resistance, while similar stacking sequence of $[90/0/\pm 45]_s$ in sample B recorded a maximum interply delamination resistance property, under maximum impact load of 2.50 kN.
- The three samples A, B and C absorbed more impact energies of 17.50, 6.25 and 14.13 J, respectively under a maximum impact load of 2.50 kN. These results were connected with their stacking sequences and consequently, the failure of their structural integrity. While, both samples E and F exhibited similar impact properties.
- A highest impact energy was absorbed by sample A, while propagation of cracks was either difficult or arrested within laminate sample B, due to their different fibre orientations of 90, 0, +45 and -45 degrees present in their stacking sequences, when compared with other samples.
- Further examination of the impacted region or centre of all the samples showed that mode/mechanism of damage depended on the stacking sequences and their fibre orientations. Admittedly, the stacking sequences of quasi-isotropic carbon reinforced epoxy composite laminates affected their impact responses. These responses determine various suitable areas of engineering applications of the CFRP composite laminates.

REFERENCES

- [1] R. S. U. Rao and T. Mahender, "Mechanical properties and optimization of processing parameters for epoxy/glass fiber reinforced composites," *Mater. Today Proc.*, 2019.
- [2] D. Dionysopoulos, C. Papadopoulos, and E. Koliniotou-Koumpia, "Effect of temperature, curing time, and filler composition on surface microhardness of composite resins," *J. Conserv.*

- Dent.*, vol. 18, no. 2, pp. 114–118, 2015.
- [3] T. D. Jagannatha and G. Harish, "Mechanical Properties of Carbon/Glass Fiber Reinforced Epoxy Hybrid Polymer Composites," *Int. J. Mech. Eng. Robot. Res.*, vol. 4, no. 2, pp. 131–137, 2015.
- [4] N. Hameed, P. A. Sreekumar, B. Francis, W. Yang, and S. Thomas, "Morphology, dynamic mechanical and thermal studies on poly(styrene-co-acrylonitrile) modified epoxy resin/glass fibre composites," *Compos. Part A Appl. Sci. Manuf.*, vol. 38, no. 12, pp. 2422–2432, 2007.
- [5] T. R. Kumar et al., "Experimental evaluation on natural composites with the incorporation of metal powders," *Mater. Today Proc.*, 2019.
- [6] H. Koushyar, S. Alavi-Soltani, B. Minaie, and M. Violette, "Effects of variation in autoclave pressure, temperature, and vacuum-application time on porosity and mechanical properties of a carbon fiber/epoxy composite," *J. Compos. Mater.*, vol. 46, no. 16, pp. 1985–2004, Dec. 2011.
- [7] X. Liu, C. A. Featherston, and D. Kennedy, "Two-level lay-up optimization of composite laminate using lamination parameters," *Compos. Struct.*, vol. 211, pp. 337–350, 2019.
- [8] G. Serhat and I. Basdogan, "Multi-objective optimization of composite plates using lamination parameters," *Mater. Des.*, vol. 180, p. 107904, 2019.
- [9] C. W. Bert, "Optimal design of a composite-material plate to maximize its fundamental frequency," *J. Sound Vib.*, vol. 50, no. 2, pp. 229–237, 1977.
- [10] H. T. Hu and B. H. Lin, "Buckling optimization of symmetrically laminated plates with various geometries and end conditions," *Compos. Sci. Technol.*, vol. 55, no. 3, pp. 277–285, 1995.
- [11] J. Körbelin, M. Derra, and B. Fiedler, "Influence of temperature and impact energy on low velocity impact damage severity in CFRP," *Compos. Part A Appl. Sci. Manuf.*, vol. 115, pp. 76–87, 2018.
- [12] M. Grasso, Y. Xu, A. Ramji, G. Zhou, A. Chrysanthou, G. Haritos, and Y. Chen, "Low-velocity impact behaviour of woven laminate plates with fire retardant resin," *Compos. Part B Eng.*, vol. 171, pp. 1-8, 2019.
- [13] Y. Hu, W. Liu, and Y. Shi, "Low-velocity impact damage research on CFRPs with Kevlar-fiber," *Compos. Struct.*, vol. 216, pp. 127–141, 2019.
- [14] D. M. Amafabia, "Analysis of the Response of Modal Parameters to Damage in CFRP Laminates using a Novel Modal Identification Method," PhD Thesis. University of Hertfordshire, 2019.
- [15] J. J. Andrew, S. M. Srinivasan, A. Arockiarajan, and H. N. Dhakal, "Parameters influencing the impact response of fiber-reinforced polymer matrix composite materials: A critical review," *Compos. Struct.*, vol. 224, pp. 1-26, 2019.
- [16] M. K. Hazzard, S. Hallett, P. T. Curtis, L. Iannucci, and R. S. Trask, "Effect of fibre orientation on the low velocity impact response of thin Dyneema® composite laminates," *Int. J. Imp. Eng.*, vol. 100, pp. 35-45, 2017.